Proceedings of ASME Turbo Expo 2011
GT2011
June 6-10, 2011, Vancouver, British Columbia, Canada

GT2011-46450

STABILITY ANALYSIS OF AN INDUSTRIAL GAS COMPRESSOR SUPPORTED BY TILTING-PAD BEARINGS UNDER DIFFERENT LUBRICATION REGIMES

Alejandro Cerda Varela*
Department of Mechanical Engineering
Technical University of Denmark
2800 Kgs. Lyngby, Denmark
Email: acer@mek.dtu.dk

Ilmar Ferreira Santos
Department of Mechanical Engineering
Technical University of Denmark
2800 Kgs. Lyngby, Denmark
Email: ifs@mek.dtu.dk

ABSTRACT

This work is aimed at theoretically study the dynamic behavior of a rotor-tilting pad journal bearing system under different lubrication regimes, namely thermohydrodynamic (THD), elastohydrodynamic (EHD) and hybrid lubrication regime. The rotor modeled corresponds to an industrial compressor. Special emphasis is put on analyzing the stability map of the rotor when the different lubrication regimes are included into the TPJB modeling. Results show that, for the studied rotor, the inclusion of a THD model is more relevant when compared to an EHD model, as it implies a reduction on the instability onset speed for the rotor. Also, results show the feasibility of extending the stable operating range of the rotor by implementing a hybrid lubrication regime.

Nomenclature

α_0	TPJB pad apperture angle.
Δs	TPJB pad thickness.
μ	oil dynamic viscosity $(Pa \cdot s)$.
ν	TPJB pad material Poisson ratio.
Ω	rotor rotational speed (rad/s).
$\bar{x}$	pad local cartesian coordinate system
$\bar{y}$	pad local cartesian coordinate system
$\bar{z}$	pad local cartesian coordinate system
ρ	oil density $\left(Kg/m^3\right)$.
ρ_s	TPJB pad material density.
$\mathbf{D}_{b1}$	damping matrix for the TPJB 1.
$\mathbf{D}_{b2}$	damping matrix for the TPJB 2.
$\mathbf{D}_g$	damping matrix for the TPJB-rotor global model.
$\mathbf{D}_r$	damping matrix for the rotor finite element model.
$\mathbf{G}_g$	gyroscopic matrix for the TPJB-rotor global model.
$\mathbf{G}_r$	gyroscopic matrix for the rotor finite element model.
$\mathbf{K}_{b1}$	stiffness matrix for the TPJB 1.
$\mathbf{K}_{b2}$	stiffness matrix for the TPJB 2.
$\mathbf{K}_g$	stiffness matrix for the TPJB-rotor global model.
$\mathbf{K}_r$	stiffness matrix for the rotor finite element model.
$\mathbf{K}_s$	stiffness matrix for the pad finite element model.
$\mathbf{M}_g$	inertia matrix for the TPJB-rotor global model.
$\mathbf{M}_r$	inertia matrix for the rotor finite element model.
$\mathbf{M}_s$	inertia matrix for the pad finite element model.
$\mathbf{V}_s$	pseudo modal matrix for the pad finite element model.
F	positioning function for injection holes $\left(m^2\right)$.
C_p	oil specific heat $(J/kg \cdot K)$.
d_0	diameter of the oil injection hole (m).
d_{ij}	damping coefficients for the TPJB.
E	TPJB pad material elasticity modulus.
EHD	elastohydrodynamic lubrication regime
f_g	TPJB-rotor global model load vector.
f_r	rotor finite element model load vector.
f_s	pad finite element model load vector.
h	oil film thickness (m).
k_c	oil thermal conductivity $(W/m \cdot K)$.
k_{ij}	stiffness coefficients for the TPJB.
L	TPJB pad width.
l_0	length of the oil injection hole (m).
n_0	number of injection holes on each pad.

*Address all correspondence to this author.

n_{flex}	number of eigenmodes included into the pseudo modal matrix for the pad finite element model.
n_s	number of pads on the TPJB.
p	oil film pressure (Pa).
P_{inj}	oil injection pressure (Pa).
q_g	TPJB-rotor global model displacements vector.
q_g^0	TPJB-rotor global model static equilibrium vector.
q_r	rotor finite element model displacements vector.
q_s	pad finite element model displacements vector.
q_s^*	modal displacements for the pad model pseudo modal reduction.
R	rotor journal radius.
R_s	TPJB pad inner radius.
T	oil temperature (°C).
t	time (s).
THD	thermohydrodynamic lubrication regime
$TPJB$	tilting pad journal bearing
U	rotor journal tangential speed (m/s).
V_{inj}	injection velocity (m/s).
x	global cartesian coordinate system
y	global cartesian coordinate system
z	global cartesian coordinate system

INTRODUCTION

Tilting pad journal bearings are commonly used in rotating machinery due to their inherent stability properties [1] [2]. Hence, an important amount of effort has been put during the last four decades in order to improve the quality and accuracy of the available models for such devices.

Lund [3] was one of the first authors to solve the Reynolds Equation for calculating theoretically the reduced dynamic coefficients of tilting-pad journal bearings. This work was later on extended by Allaire [4] in order to calculate the complete set of dynamic coefficients for the bearing. Malcher [5] and Klumpp [6] investigated theoretically and experimentally the behavior of the dynamic coefficients on the basis of advanced experiments. Jones and Martin [7] studied theoretically the influence of bearing geometry on the steady-state and dynamic behavior of these bearings. Springer [8, 9], Rouch [10] and Parsell et al. [11] investigated theoretically the dynamic properties of these bearings for predicting rotor instabilities. Ettles [12] included pivot flexibility and thermal effects in one model and concluded that thermal effects can reduce the bearing damping properties. Such damping reduction effect was also observed when including pad flexibility in a simplified model [13] and when using the finite element method to include both pad flexibility and pivot stiffness [14, 15]. Dmochowski [16] investigated theoretically as well as experimentally the behaviour of damping and stiffness reduced coefficients as a function of the excitation frequency taking into consideration the influence of pivot flexibility.

The tilting pad-journal bearings models have been expanded consistently from their basic hydrodynamic formulation to include other effects, reaching nowadays a thermoelastohydrodynamic formulation [17]. Also, experimental and theoretical effort has been put on studying the feasibility of achieving an active lubrication regime [18–21], where the TPJB can be used to apply controlled forces over the rotor, enabling to modify its dynamic behavior.

The rotor-bearing stability properties are strongly dependent on the bearing dynamic coefficients [22], due to their significant contribution to the stiffness and specially damping characteristics of the overall system. Hence, the stability analysis of a rotor supported by TPJBs is strongly dependent on the modeling of the bearings themselves, hence on the lubrication regime assumed.

The main original contribution of this paper is not focused on the actual modeling of the TPJB-rotor system, but on the comparison of the effect of different lubrication regimes over the rotor stability analysis. This work is aimed at investigating the stability of an industrial compressor supported by TPJBs. Three lubrication regimes (EHD, THD, hybrid) are separately imposed, in order to clearly identify their effect on the stability of the global system.

MODELING

For the modeling of the rotor-bearing system, this paper relies heavily on previous work on the subject. Hence, the mathematical models used to describe the behavior of the different components of the system are only presented on a brief way, for the sake of completeness of this paper. For a more complete description on the way such models were obtained, the reader should refer to the given references.

Modified Reynolds Equation

The theoretical stability analysis of an industrial rotor requires the existence of a mathematical model, capable of representing accurately the inertia, stiffness and damping properties of the studied system. The inclusion of the bearings into the model requires an adequate modeling of their stiffness and damping properties. Such properties, in the case of tilting pad journal bearings, depend on the pressure field developed within the oil film during the operation of the bearing. Hence, a suitable model for the oil film behavior is required.

The fluid film behavior in the land surfaces of finite oil film bearing is described by the Reynolds equation, deduced by using the Navier-Stokes and continuity equations, considering a laminar flow where the inertia of the fluid and the shear viscous forces in the radial direction are neglected. The non-slip boundary condition is applied at the surface of the rotor and the pads. The basic formulation for the Reynolds equation was extended [18] in order to include the effect of injecting oil into the bearing clearance using an orifice drilled through the surface of the pad, obtaining the Modified Reynolds Equation as shown in Eqn. (1):

$$\frac{\partial}{\partial \overline{y}}\left(\frac{h^3}{\mu}\frac{\partial p}{\partial \overline{y}}\right)+\frac{\partial}{\partial \overline{z}}\left(\frac{h^3}{\mu}\frac{\partial p}{\partial \overline{z}}\right)-\frac{3}{\mu l_0}\sum_{i=1}^{n_0}F_i\left(\overline{y},\overline{z}\right)\cdot p = 6U\frac{\partial h}{\partial \overline{y}}-12\frac{\partial h}{\partial t}-\frac{3}{\mu l_0}\sum_{i=1}^{n_0}F_i\left(\overline{y},\overline{z}\right)\cdot P_{inj} \tag{1}$$

where $F_i\left(\overline{y},\overline{z}\right)$ is defined as follows:

$$\begin{aligned} F_i\left(\overline{y},\overline{z}\right) &= \frac{d_0^2}{4}-\left(\overline{y}-\overline{y_i}\right)^2-\left(\overline{z}-\overline{z_i}\right)^2 \\ &\quad ,\text{ if } \left(\overline{y}-\overline{y_i}\right)^2-\left(\overline{z}-\overline{z_i}\right)^2 \leq \frac{d_0^2}{4} \\ F_i\left(\overline{y},\overline{z}\right) &= 0 \\ &\quad ,\text{ if } \left(\overline{y}-\overline{y_i}\right)^2-\left(\overline{z}-\overline{z_i}\right)^2 \geq \frac{d_0^2}{4} \end{aligned} \tag{2}$$

A number of publications [19–21] on the subject of actively lubricated tilting pad journal bearings base the modeling of the oil film under a hybrid lubrication regime on Eqn. (1). The references included here only correspond to the earlier work on the subject. It can be seen that the function $F_i\left(\overline{y},\overline{z}\right)$ is related to the orifices position along the pad surface, given by the coordinates $\left(\overline{y}_i,\overline{z}_i\right)$, and the orifices diameter d_0. For a passive TPJB, $F_i\left(\overline{y},\overline{z}\right)$ is equal to zero, hence the term P_{inj} corresponding to the oil injection pressure, vanishes.

From Eqn. (1), it can be seen that pressure field $p\left(\overline{y},\overline{z}\right)$ developed in the oil film is a function of rotor rotational speed ($U = \Omega\cdot R$), the oil viscosity μ, the oil film thickness h, which is a function of rotor journal position and the rotation of each bearing pad, and the injection pressure P_{inj} and injection hole geometry , in the case of a hybrid lubrication regime. Hence, this basic model can be extended in order to include other effects which vary any of these parameters, entailing a modification of the pressure profile and the resulting forces over the rotor, with the subsequent change in the behavior of the TPJBs-rotor system.

Thermohydrodynamic Model

The previously defined model for the oil film behavior correspond to an isothermal formulation for the problem. It means that the effect of the temperature build up due to the viscous forces generated across the oil film during the operation of the bearing and the subsequent reduction of the oil film viscosity is neglected. If such effect is included into the modeling, then a THD model is obtained, as explained in [23, 24]. To do so, one must solve the energy equation, stated in Eqn. (3), in order to obtain the temperature field $T\left(\overline{y},\overline{z}\right)$ across the oil film as a function of the bearing gap h.

$$\begin{aligned} &\rho C_p h\frac{\partial T}{\partial t}+k_c h\frac{\partial^2 T}{\partial \overline{y}^2}+k_c h\frac{\partial^2 T}{\partial \overline{z}^2}+k_c\left.\frac{\partial T}{\partial \overline{x}}\right|_0 F_i \\ &+\left(\frac{\rho C_p h^3}{12\mu}\frac{\partial p}{\partial \overline{y}}-\frac{\rho C_p U h}{2}\right)\frac{\partial T}{\partial \overline{y}}+\frac{\rho C_p h^3}{12\mu}\frac{\partial p}{\partial \overline{z}}\frac{\partial T}{\partial \overline{z}} \\ &\rho C_p\left(V_{inj}-\frac{\partial h}{\partial t}\right)\left(T-T_{inj}\right)=\frac{4}{3}\frac{\mu}{h}\left(V_{inj}-\frac{\partial h}{\partial t}\right)^2 \\ &p\left(V_{inj}-\frac{\partial h}{\partial t}\right)-U^2\frac{\mu}{h}-\frac{h^3}{12\mu}\left[\left(\frac{\partial p}{\partial \overline{y}}\right)^2+\left(\frac{\partial p}{\partial \overline{z}}\right)^2\right] \end{aligned} \tag{3}$$

It must be noted that the THD model presented here corresponds to an adiabatic solution, meaning that no heat transfer takes place between the oil and the pads. Here, the injection velocity profile V_{inj} is determined as a completely developed laminar flow inside the injection orifice, using the following expression:

$$V_{inj}\left(\overline{y},\overline{z}\right)=-\frac{1}{4\mu l_0}\left(P_{inj}-p\right)\cdot\sum_{i=1}^{n_0}F_i\left(\overline{y},\overline{z}\right) \tag{4}$$

Once Eqn. (3) is solved and the temperature field $T\left(\overline{y},\overline{z}\right)$ is obtained, one can calculate the viscosity across the oil film as a function of such temperature field.

Elastohydrodynamic Model

In this work, the inclusion of the pad flexibility is done following a pseudo-modal reduction scheme, as exposed firstly in [25] and then used in [26, 27] to study the EHD regime with hybrid lubrication. The pads are modeled using the finite element method. By using this method, the mathematical model for the pads is defined as:

$$\mathbf{M}_s\ddot{q}_s+\mathbf{K}_s q_s = f_s \tag{5}$$

where q_s correspond to the degrees of freedom for each node of the finite element model, $\mathbf{M}_s$ and $\mathbf{K}_s$ correspond to the inertia and stiffness matrix for the pads, obtained using the finite element method, and f_s represent the loads over the pads due to the pressure profile in the oil film. By calculating the pseudo-modal matrix $\mathbf{V}_s$ containing on its columns some of the eigenmodes of the pads, one can rearrange Eqn. (5) as follows:

$$\begin{aligned} \mathbf{V}_s^T\mathbf{M}_s\mathbf{V}_s\ddot{q}_s^*+\mathbf{V}_s^T\mathbf{K}_s\mathbf{V}_s q_s^* &= \mathbf{V}_s^T f_s \\ q_s &= \mathbf{V}_s q_s^* \end{aligned} \tag{6}$$

By using the reduction scheme exposed in Eqn. (6), one ends working with a reduced system defined by the modal coordinates vector q_s^*, where there are as many degrees of freedom as eigenmodes were included into the modal matrix $\mathbf{V}_s$. It corresponds to a pseudo-modal reduction, since only the eigenmodes which are relevant are included into the analysis. If only the first eigenmode is included, then a rigid pad model is established, and the corresponding modal coordinate measures the rotation of the pad around the pivot. The use of higher eigenmodes enables to include the flexibility of the pads into the results.
Since it is always possible to obtain the "true" displacements of the pads q_s based on the modal displacements q_s^*, one can determine the oil film thickness h in order to solve Reynolds Equation. Hence, the link between pad deformation and pressure profile and the resulting loads over the rotor and pads is established. The use of the pseudo-modal reduction is specially convenient when it comes to obtain the dynamic coefficients of the TPJB. If one uses the full finite element model of the pads in order to obtain the dynamic coefficients of the bearing, it is necessary to perturb analytically or numerically every single degree of freedom associated with the finite element model. By using the pseudo modal reduction scheme, only the modal coordinates q_s^* are perturbed, reducing the workload and making the results more manageable and easier to interpret on a physical way.

TPJB Dynamic Coefficients

The inclusion of the TPJBs into the global rotor model is performed by calculating the dynamic coefficients associated with the bearings. Firstly introduced by [3] to obtain synchronously reduced dynamic coefficients and then extended by [4] to calculate the complete set of dynamic coefficients, the concept of the dynamic coefficients has become a cornerstone among the tools employed for analyzing the dynamic behavior of a rotor mounted over oil film bearings. It allows the analyst to avoid the computationally expensive operation of solving the Reynolds Equation to determine the pressure profile and the resulting loads over the rotor journal and bearing pads. Instead, the behavior of such loads is linearized around the static equilibrium of the system, using a first order approximation. Hence, one can define the stiffness and damping coefficients for the TPJB as follows:

$$k_{ij} = \frac{\partial F_i}{\partial \delta_j}$$
$$d_{ij} = \frac{\partial F_i}{\partial \dot{\delta}_j} \tag{7}$$

where δ_j corresponds to the degrees of freedom associated with the journal-TPJB system. If a rigid pad model is used, then $i, j = 1, ..., 2+n_s$, including the two translational degrees of freedom of the rotor journal and the rotations of each pad. If a flexible pad model is used, then $i, j = 1, ..., 2+n_s \cdot n_{flex}$, where n_{flex} correspond to the number of modes for each pad included into the analysis, according to the pseudo modal reduction scheme. If $n_{flex} = 1$, then the flexible model is reduced to a rigid pad model.
Synchronously reduced coefficients are calculated in order to describe the general behavior of the stiffness and damping properties of the bearing when the different lubrication regimes are included. For analyzing the stability of the TPJBs-rotor system, the complete set of dynamic coefficients are used. Some results regarding the stability of the TPJB - rotor system are also obtained using the synchronously reduced dynamic coefficients of the bearings, in order to observe their effect into the overall stability behavior of the studied system.

Rotor Modeling

The finite element method is employed to model the rotor, using shaft elements, as proposed by [28]. Proportional damping is used in order to model the energy dissipation across the rotor. The proportional damping parameters are tuned in order to obtain a damping ratio equal to 0.001 for the two first natural frequencies of the rotor on free-free boundary conditions.
By using this method, the system can be represented mathematically as follows:

$$\mathbf{M}_r \ddot{q}_r + (\mathbf{D}_r - \Omega \mathbf{G}_r)\dot{q}_r + \mathbf{K}_r q_r = f_r \tag{8}$$

In Eqn. (8), q_r represent the degrees of freedom of the nodes corresponding to the finite shaft model of the rotor, $\mathbf{M}_r$ is the rotor inertia matrix, $\mathbf{D}_r$ is the proportional damping matrix, $\mathbf{G}_r$ is the gyroscopic matrix and $\mathbf{K}_r$ is the rotor stiffness matrix. Related to the loading term f_r, for this analysis the only loading applied to the system corresponds to the static load due to the weight of the rotor.

Stability Analysis for the TPJBs-Rotor System

So far, the mathematical models for the TPJBs and the rotor have been exposed separately. In order to analyze the stability, one must couple such models into a global system, which includes the degrees of freedom of the rotor and the bearing pads. By doing so, the model for the global system is defined as:

$$\mathbf{M}_g \ddot{q}_g + (\mathbf{D}_g - \Omega \mathbf{G}_g)\dot{q}_g + \mathbf{K}_g q_g = f_g$$
$$\text{where} \quad q_g = \{q_r \; q_s^*\}^T \tag{9}$$

The degrees of freedom for the global system q_g are defined by the rotor model degrees of freedom q_r and by the pads degrees of freedom q_s^*, derived from the pseudo modal reduction. If a rigid pad model is utilized, then there are n_s degrees of freedom associated with pads, corresponding to the rotations around the pivots. If a flexible model is used, then there are $n_s \cdot n_{flex}$ degrees of freedom associated with the pads, with the additional degrees of freedom related to the pad deformations. According to Eqn. (9), in order to analyze the system it becomes necessary to define the global mass, damping and stiffness matrices. The use of the dynamic coefficients for representing the TPJBs in the global system enables to do such coupling in a straightforward fashion. The procedure followed to analyze the stability of the rotor system is depicted as follows:

1. Set a desired rotational speed for the rotor Ω
2. Using a Newton Raphson scheme, determine the static equilibrium position for the global system q_g^0.The Reynolds equation is solved in order to determine the pressure field on each pad. Then, direct integration of the pressure field is employed in order to determine the forces over the rotor and the pads surface by the fluid film.
3. For the determined equilibrium position, using a perturbation method, one calculates the dynamic stiffness and damping coefficients for each TPJB, related to the rotor journal degrees of freedom and the pads degrees of freedom coming from the pseudo modal reduction scheme. By doing so, stiffness $\mathbf{K}_{b1}$,$\mathbf{K}_{b2}$ and damping matrices $\mathbf{D}_{b1}$,$\mathbf{D}_{b2}$ are obtained for each bearing.
4. By assembling the stiffness and damping matrix from the rotor finite element model $\mathbf{K}_r$ and $\mathbf{D}_r$ with the ones coming from the bearings stiffness coefficients $\mathbf{K}_{b1}$,$\mathbf{K}_{b2}$ and damping coefficients $\mathbf{D}_{b1}$,$\mathbf{D}_{b2}$, one obtains the global matrices $\mathbf{K}_g$ and $\mathbf{D}_g$. As for the global mass matrix $\mathbf{M}_g$, only the inertia coming from the rotational degrees of freedom of the pads is included into the model.
5. Having the global matrices completely defined, including both the presence of the rotor and the bearing pads, it is possible to calculate the eigenvalues and eigenmodes for the global system. The sign of the real part of the obtained eigenvalues is used to determine the stability of the system. If positive, it means that the rotor system presents unstable behavior.

TABLE 1. TPJB CHARACTERISTICS

Parameter	Value	Units
Journal Radius (R)	50.800	mm
Number of pads (n_s)	5	-
Pad inner Radius (R_s)	50.921	mm
Pad aperture angle (α_0)	60	deg
Angular position pivot pad #1	60	deg
Angular position pivot pad #2	132	deg
Angular position pivot pad #3	204	deg
Angular position pivot pad #4	276	deg
Angular position pivot pad #5	348	deg
Offset	0.6	-
Pad width (L)	44.450	mm
Pad thickness (Δs)	10.312	mm
Pad material elasticity modulus (E)	200	GPa
Pad material Poisson ratio (ν)	0.3	-
Pad material density (ρ_s)	7800	Kg/m^3
Injection orifice length (l_0)	5.0	mm
Injection orifice diameter (d_0)	5.0	mm
Number of orifices per pad (n_0)	1,2	-
Assembled bearing gap (h_0)	102	μm
Oil viscosity (40°C)) (μ)	0.028	Pa s
Oil viscosity (80°C)) (μ)	0.007	Pa s
Oil density (ρ)	863.5	Kg/m^3
Oil specific heat (C_p)	1900	$J/kg \cdot K$
Oil thermal conductivity (k_c)	0.13	$W/m \cdot K$
Oil supply temperature	50	°C

CASE ANALYSIS: INDUSTRIAL COMPRESSOR MODELING

In this section, the results obtained by using the previously defined mathematical model for studying an industrial case are presented. The system modeled corresponds to an industrial rotor system. Namely, the rotor corresponds to a gas compressor, composed of five impellers. It weighs 391 Kg, and it operates normally within the range of 6942 RPM and 10170 RPM. The rotor is supported by two identical tilting pad journal bearings. Figure 1 shows the finite element model of such rotor, depicting also the location of the TPJB and the reference systems used on this study. The loading due to the rotor weight acts on the negative y direction, hence pad #4 becomes the most heavily loaded one. The impellers, seals and other machine elements are considered as rigid discs and are incorporated into the model by adding

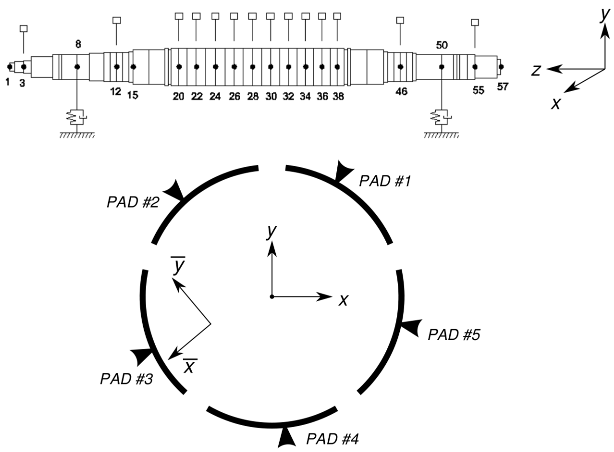

FIGURE 1. MECHANICAL MODEL OF THE COMPRESSOR BY SHAFT ELEMENTS; GLOBAL COORDINATE SYSTEM (x,y,z) AND PAD LOCAL COORDINATE SYSTEM $(\bar{x},\bar{y},\bar{z})$ USED FOR THE STUDY

inertia to the respective nodes. Hence, in the model, the impellers are at nodes 20,24, 28, 32 and 36. Bushes are at nodes 22,26, 30, and 34. A thrust disk sleeve is located at node 3. A balance piston is located at node 38. Seal bushes are located at nodes 12 and 46. Coupling is at node 55.
As for the TPJBs, they are located at nodes 8 and 50. From now on, the bearing located at node 8 will be referred as "bearing 1" and the one located at node 50 as "bearing 2". Tab.1 depicts all the parameters that define the geometry of such bearings.

Numerical results

The obtained results are presented in a way that enables to compare the effect of including different lubrication regimes models for the TPJBs on the overall behavior of the studied rotor - bearings system. Hence, only one effect is studied at the time, in order to identify clearly the consequences of including it into the modeling. The lubrication regimes to be studied are:

1. *Elastohydrodynamic lubrication regime (EHD)* : in this section, the flexibility of the pads is included into the model by using the pseudo modal reduction method. The oil film is modeled using the Reynolds Equation. No thermal effects are included into the oil film model. The bearings work in passive configuration, meaning that no oil injection into the bearing clearance is taking place.
2. *Thermohydrodynamic lubrication regime (THD)* : in this section, the temperature build-up generated on the bearings oil film due to rotor operation is modeled using the THD model exposed previously. No pad flexibility effects are included, and no oil is injected into the bearing clearance.

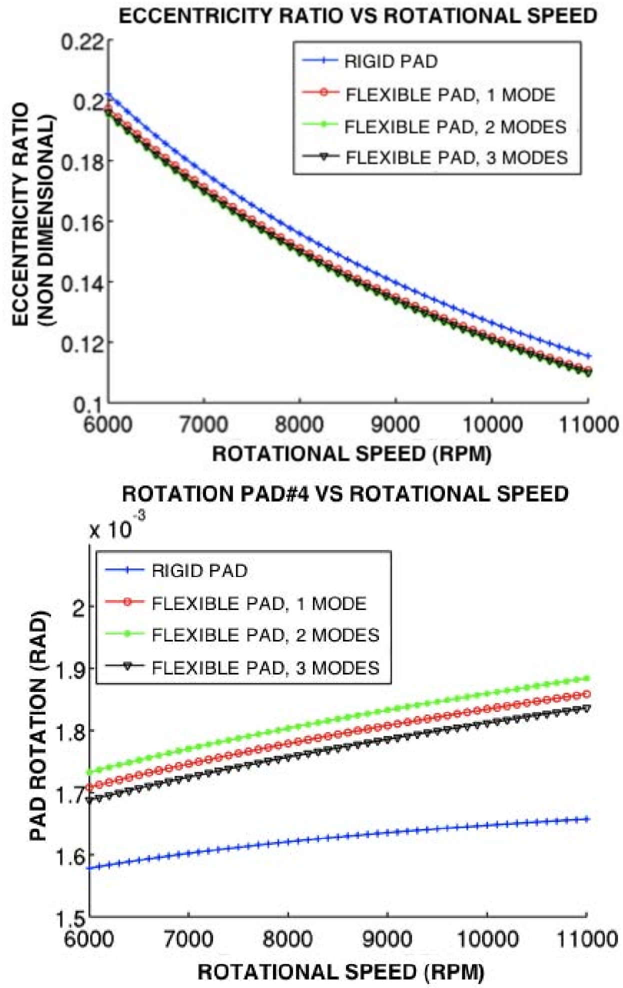

FIGURE 2. STATIC EQUILIBRIUM POSITION FOR BEARING 1, AS A FUNCTION OF THE ROTATIONAL SPEED; RESULTS FOR THE ECCENTRICITY RATIO OF THE ROTOR JOURNAL AND THE ROTATION OF PAD # 4

3. *Hybrid lubrication regime* : in this section, the effect of injecting oil at different pressures into the bearing clearance is included. No thermal effects and no pad flexibility effects are taken into account.

The results analyzed include: static equilibrium position for the TPJB pads and rotor journals, dynamic coefficients for the TPJBs, stability map for the rotor-bearings system. Regarding the equilibrium position results, the ecentricity ratio is calculated as the ratio between shaft journal displacement and the assembled bearing gap (h_0). The results obtained are presented as a function of the rotor rotational speed in the range between 6000 RPM and 11000 RPM.

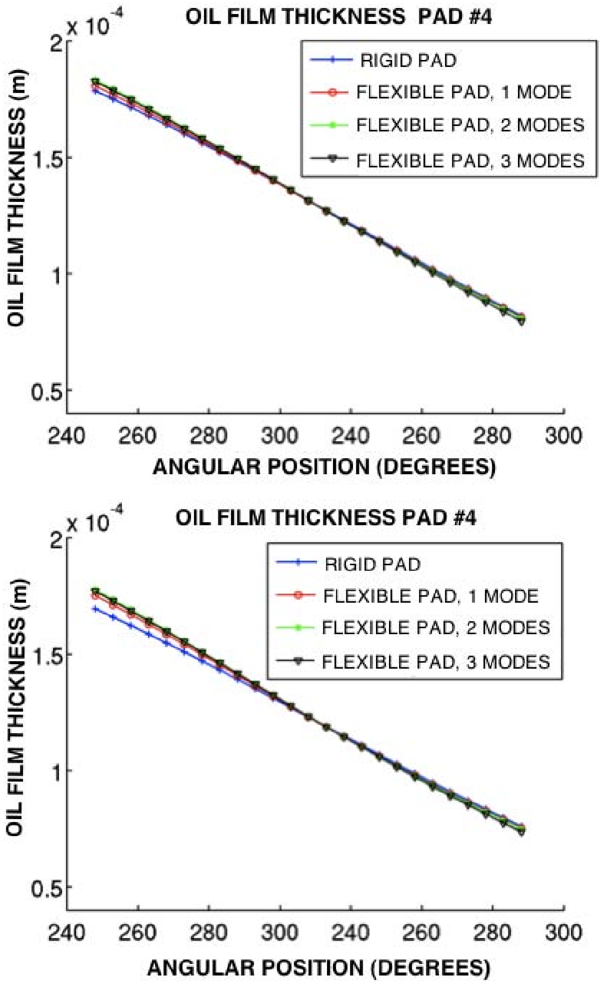

FIGURE 3. OIL FILM THICKNESS FOR BEARING 1 PAD #4 AT EQUILIBRIUM POSITION; COMPARISON OF RESULTS FOR 6000 RPM (UPPER) AND 11000 RPM (LOWER). RESULTS OBTAINED AT $\overline{Z} = 0$

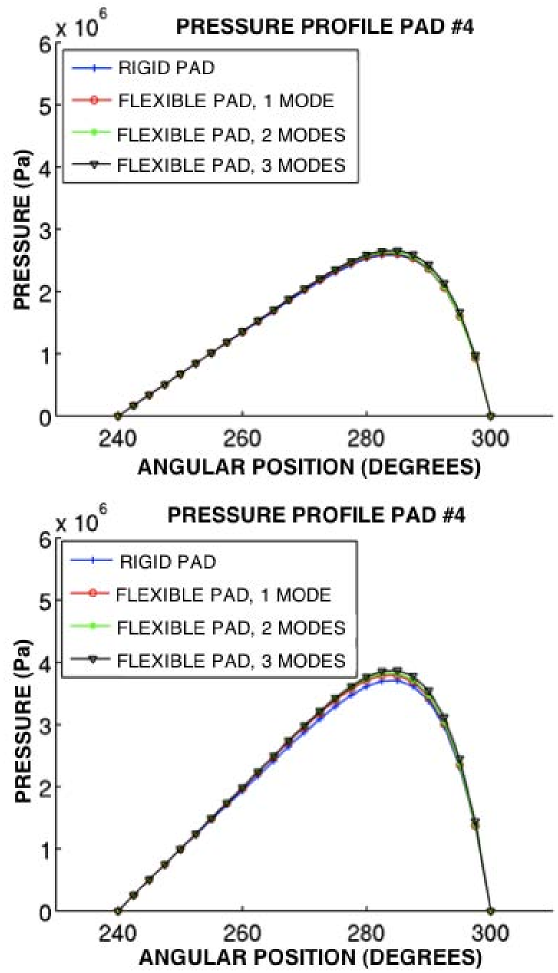

FIGURE 4. PRESSURE PROFILE AT EQUILIBRIUM POSITION FOR BEARING 1 PAD #4; COMPARISON OF RESULTS FOR 6000 RPM (UPPER) AND 11000 RPM (LOWER). RESULTS OBTAINED AT $\overline{Z} = 0$

Elastohydrodynamic regime results The behavior of the pressure field generated in a TPJB oil film is influenced, among other over variables, by the bearing clearance, namely, the distance existing between the pad and the journal surface. Such parameter is included into the Reynolds Equation by the h parameter. When one considers the pads to be rigid, such parameter is only a function of the journal position and the pads angular rotation. However, if the pads are considered as flexible elements, then the clearance is also a function of the deformations on the pads due to the load exerted over them by the oil film pressure. Hence, one can expect that the pressure field, and the resulting forces over the rotor are affected by the pad flexibility effect. The question to be answered is how relevant is the inclusion of such effect into the overall modeling of the rotor dynamic behavior.

Firstly, one can compare the static equilibrium position achieved by the rotor journal and the bearing pads when including the flexibility of the pads into the modeling. Fig.2 shows the eccentricity ratio and rotation of pad #4 as a function of the rotation speed of the rotor, for the rigid and the flexible pads. It can be seen that, by including the flexibility of the pads, the eccentricity ratio decreases over the studied rotational speed, and the tilt angle of the pad becomes higher. Hence, the equilibrium position of the system is altered. Since for all cases the same load is applied over the bearing (the one due to the weight of the rotor), one can state that by including the pad flexibility the bearing system actually becomes stiffer, in other words, for the same applied load over the rotor journal a lower displacement is obtained. Although the fact that by adding extra flexibility into

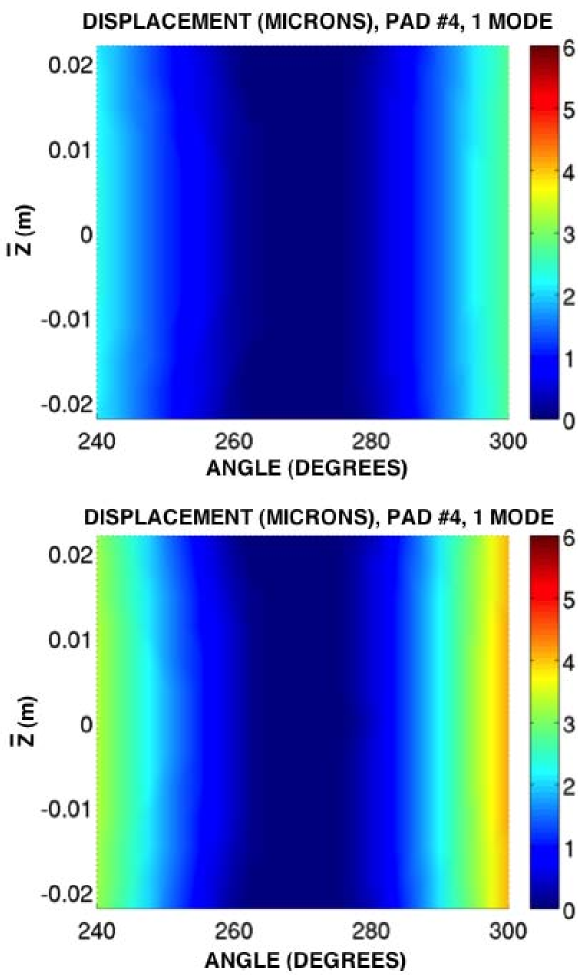

FIGURE 5. DEFORMATION OF BEARING 1 PAD#4 AT EQUILIBRIUM POSITION; COMPARISON OF RESULTS FOR 6000 RPM (UPPER) AND 11000 RPM (LOWER)

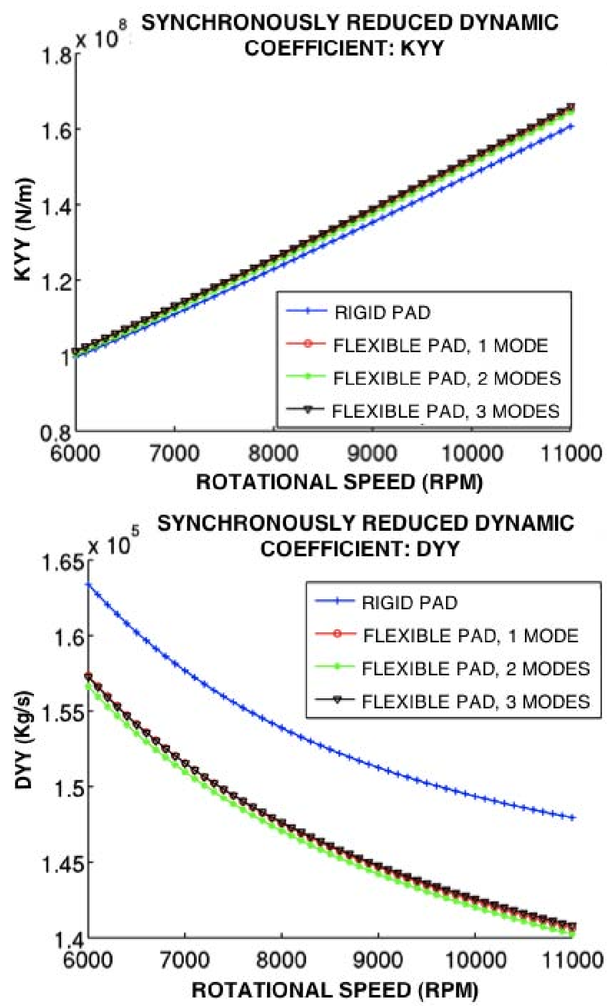

FIGURE 6. SYNCHRONOUSLY REDUCED DIRECT STIFFNESS AND DAMPING COEFFICIENTS FOR BEARING 1, VERTICAL DIRECTION: COMPARISON BETWEEN RIGID PADS AND FLEXIBLE PADS WITH DIFFERENT NUMBER OF FLEXIBLE MODES INCLUDED

the pads model entails a stiffer bearing system may seem unnatural at first glance, one must understand that the overall stiffness of the bearing system is highly influenced by the stiffness of the oil film. Such stiffness is a function of the bearing clearances, determined by the system equilibrium position and deformation of the pads. Hence, since the effect of the pad flexibility is to alter the bearing clearance, the stiffness of the oil film is modified, implying that the overall system becomes stiffer.

The previous statement can be confirmed by taking a look at Fig. 3 and Fig. 4. One can see that the inclusion of the pad flexibility entails a variation of the oil film thickness, which also implies that the pressure profile is modified. Such change is a consequence of the system new equilibrium position (rotor journal position and pad tilt) and the deformation of the pads. It is also seen that such effect is stronger for higher rotational speed, which is consistent on the higher pressure generated when operating at a higher speed, which implies higher deformation of the pads.

From the results presented so far, one can also note that the inclusion of mode 2 and 3 into the flexible model of the pad does not entail a relevant change in the behaviour of the system, when compared to the effect of just including the first flexible mode. It means that the first flexible mode is dominating when it comes to obtaining the deformed shape of the pad under load. The deformation of the surface of the pad due to the first flexible mode can be seen in Fig. 5. It can be seen that the maximum deformation of the pad is about a 3% of the oil film minimum thickness, and it is obtained toward the edge of the pads. No deformation

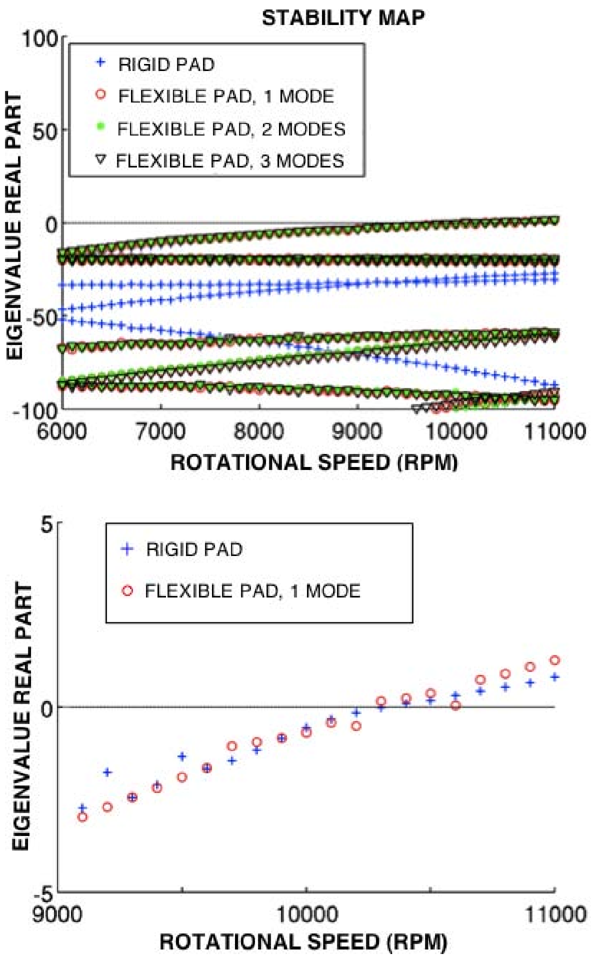

FIGURE 7. STABILITY MAP FOR THE COMPRESSOR; COMPARISON BETWEEN RIGID PADS AND FLEXIBLE PADS MODEL, FOR DIFFERENT NUMBER OF MODES (LOWER FIGURE DETAILS THE INSTABILITY ONSET ZONE)

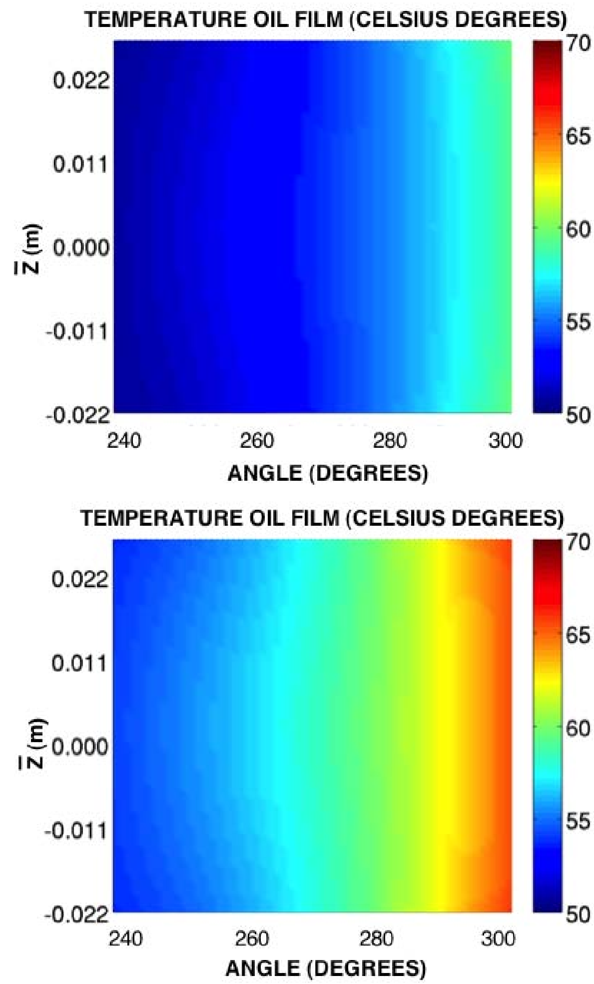

FIGURE 8. OIL FILM TEMPERATURE FOR BEARING 1 PAD#4 AT EQUILIBRIUM POSITION; COMPARISON OF RESULTS FOR 6000 RPM (UPPER) AND 11000 RPM (LOWER)

is obtained around the pivot of the pad, due to the fact that the included mode corresponds to a pure bending mode, where no pad surface deformation is included and where the nodes around the pivot have their displacement restricted. As expected, the deformation of the pads due to the first flexible mode is larger for higher rotational speed, and the deformations implies that, in practice, the curvature radius of the pads are increased. Such effect implies a higher "effective" preload factor into the system, which support the "stiffening" effect commented when looking at the results shown in Fig. 2.

The link between the TPJB "local" behavior, discussed so far, and the overall dynamic behavior of the rotor system comes from the dynamic coefficients, used to represent the bearing into the dynamic model. In order to present this information in a compact way, the synchronously reduced dynamic coefficients are obtained for the studied TPJB. The direct stiffness and damping coefficients in the vertical direction of bearing 1, as a function of the rotational speed, are shown in Fig. 6. On these results, the conclusions obtained so far from the equilibrium positions, oil film thickness and pressure profiles of the studied bearing are confirmed. First, one can note convergence behavior on the results obtained when including just the first flexible mode and the two other modes. Secondly, it can be seen that the results from the rigid pad and the flexible pad model approach each other for lower rotational speeds. This is consistent with relationship between rotational speed, pressure profile and deformations of the pads. Thirdly, it can be noted that the inclusion of the pad flexibility generates a stiffening of the overall bearing system. Lastly, one can see a reduction of the damping coefficient of the bear-

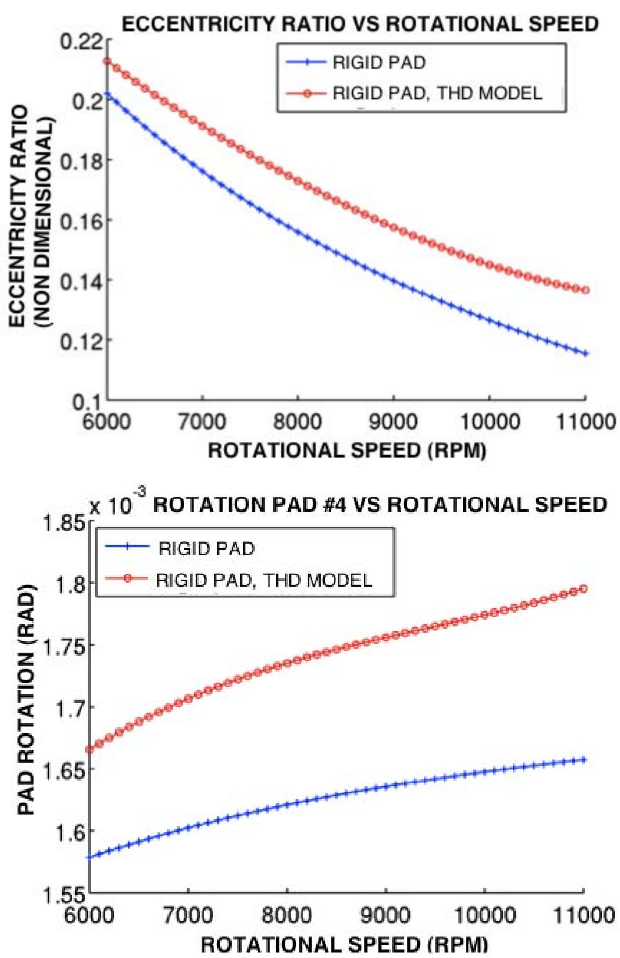

FIGURE 9. STATIC EQUILIBRIUM POSITION FOR BEARING 1, AS A FUNCTION OF ROTATIONAL SPEED; RESULTS FOR ECCENTRICITY RATIO OF THE ROTOR JOURNAL AND THE ROTATION OF PAD #4

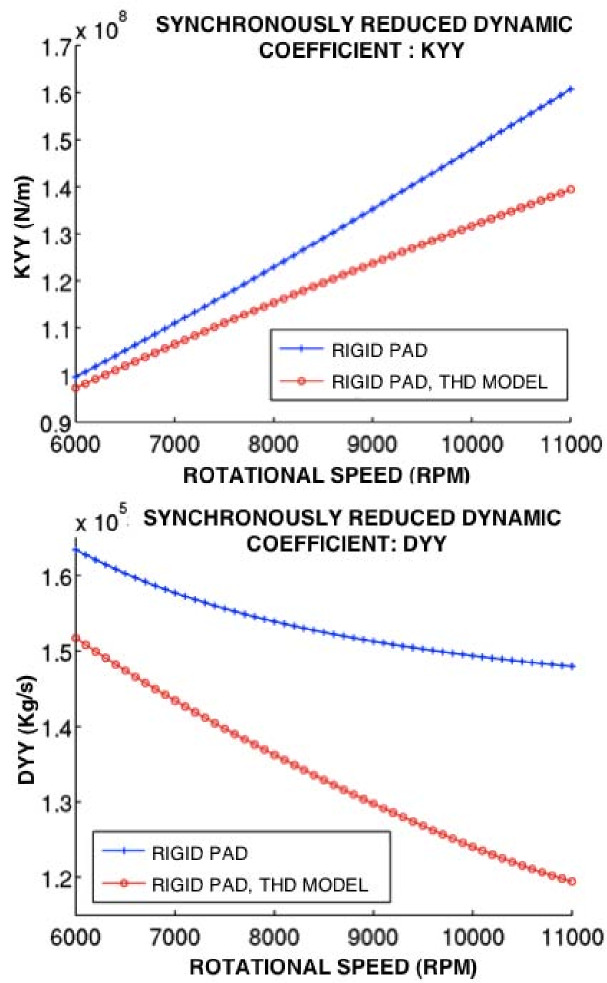

FIGURE 10. SYNCHRONOUSLY REDUCED DIRECT STIFFNESS AND DAMPING COEFFICIENTS FOR BEARING 1, VERTICAL DIRECTION; EFFECT OF INCLUDING THD MODEL

ing when increasing the rotational speed and when including the flexibility of the pads. This result fits with the stiffening effect observed when increasing the rotational speed and when including the flexibility of the pads.

The stability map obtained using the TPJB complete dynamic coefficients is shown in Fig. 7. Results are shown for the rigid and flexible pad assumption. Once again, convergence on the behavior of the system when incorporating the different flexible modes for the pads is observed. It can be noted that the instability onset speed is not modified in a noticeable way by the inclusion of modes 2 and 3, when compared to the results obtained when only including the first flexible mode. When comparing the results obtained assuming rigid pads with those including the first flexible mode, it can be seen that the change in the instability onset speed is almost negligible. Putting this result in perspective, it means that for the specific rotor under study, under its particular operating conditions of load and speed, the effect of including the flexibility of the pads is not relevant when it comes to analyzing the stability of the rotor system.

Thermohydrodynamic regime results The viscous friction forces generated across the TPJB oil film induce a temperature build up of the oil. Since the oil viscosity is a function of the temperature, such property of the lubricant is modified when including a thermal model in the modeling of the oil film behavior. From the Reynolds equation, it is evident that any change in the viscosity of the lubricant induces changes in the pressure profiles, hence in the overall behavior of the bearing.

By solving the THD model, one obtains non-uniform temperature and viscosity values for the oil film. Such results are

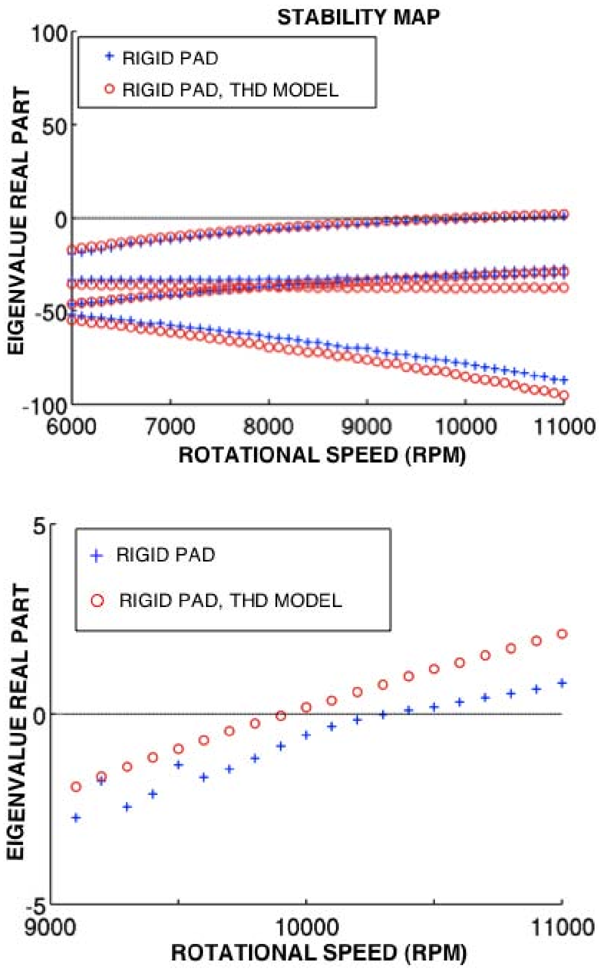

FIGURE 11. STABILITY MAP FOR THE COMPRESSOR; EFFECT OF INCLUDING THE THD MODEL FOR THE OIL FILM (LOWER FIGURE DETAILS THE INSTABILITY ONSET ZONE)

shown in Fig. 8. From those results, it becomes clear the increase in the oil film temperature and the decrease of the oil viscosity for a higher rotational speed. Also, it can be seen that the highest temperature values (and lower viscosity) are obtained in the area where the oil film thickness is lower.

When looking at Fig. 9, one can see that the change in viscosity due to the oil temperature build up has clear effects on the equilibrium position of the bearing. The eccentricity ratio becomes higher for all rotational speeds analyzed, meaning the rotor journal achieves a lower equilibrium position. Also, the tilt of the pad becomes higher. This can be explained when analyzing the Reynolds Equation. In order to equilibrate the static load applied over the rotor journal, a pressure profile must be obtained on each pad. The pressure profile, on static conditions, is a function of the gradient of the oil film thickness in the journal sliding

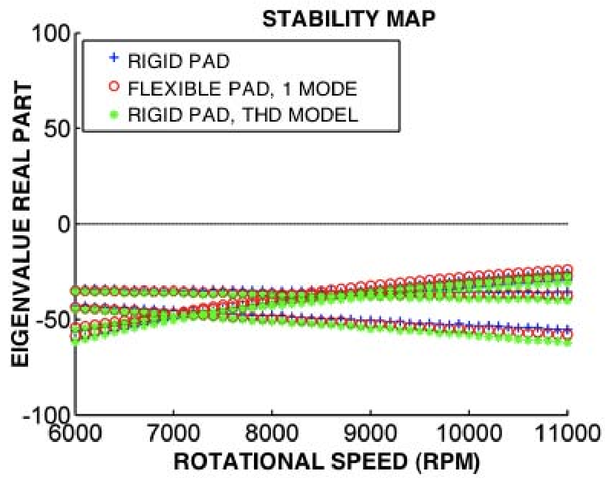

FIGURE 12. STABILITY MAP FOR THE COMPRESSOR, CALCULATED USING THE TPJBs SYNCHRONOUSLY REDUCED DYNAMIC COEFFICIENTS FOR DIFFERENT LUBRICATION REGIMES

direction. Since the viscosity is lower for higher temperatures, a higher oil film thickness gradient is necessary in order to generate the required pressure profile. This is obtained by a higher eccentricity and a higher tilt of the pads.

The change induced over the oil film thickness and the pressure profile by the oil film thermal effects entails a change in the bearing dynamic coefficients, as shown in Fig. 10. The overall effect consists in a reduction of the bearing stiffness and damping properties. Such reduction becomes more important as one increases the rotational speed, which is consistent with the fact that shear forces across the fluid film are function of the rotational speed of the rotor.

When looking at the stability map shown in Fig. 11, it becomes clear that for the studied rotor, not including the thermal effects on the oil film modeling would induce an overestimation of the stability of the rotor. This is a relevant result, moreover because the load and operating speed of the studied system can be considered ”low”.

Stability analysis using the synchronously reduced dynamic coefficients for the bearings The stability results presented so far were obtained using the full set of dynamic coefficients to include the bearings into the rotor model. If one uses the synchronously reduced dynamic coefficients to represent the bearings, the results obtained for the stability map are shown in Fig. 12. By comparing these results with the ones already presented in Fig. 7 and Fig. 11, it becomes evident that such approach induces an important overestimation of the stable operating range of the studied system, when compared to the results obtained using the full set of bearing dynamic coefficients.

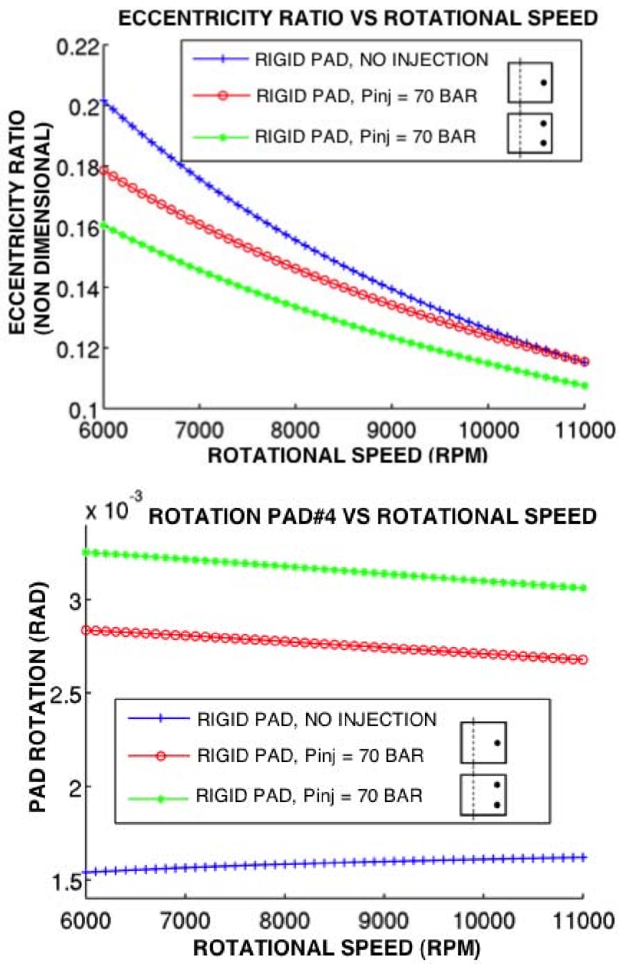

FIGURE 13. STATIC EQUILIBRIUM FOR BEARING 1, AS A FUNCTION OF ROTATIONAL SPEED; RESULTS FOR THE ECCENTRICITY RATIO OF THE ROTOR JOURNAL AND THE ROTATION OF PAD#4, EFFECT OF OIL INJECTION FOR TWO CONFIGURATIONS

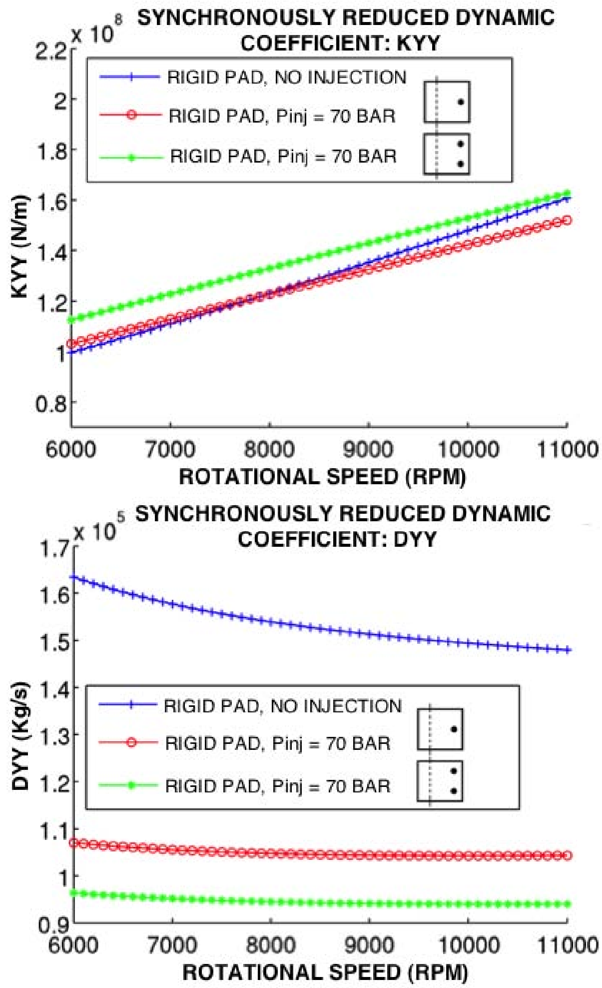

FIGURE 14. SYNCHRONOUSLY REDUCED DIRECT STIFFNESS AND DAMPING COEFFICIENTS FOR BEARING 1, VERTICAL DIRECTION; EFFECT OF OIL INJECTION FOR TWO CONFIGURATIONS

Hybrid lubrication regime results When speaking of a hybrid lubrication regime, one refers to a system where high pressurized oil is injected through an orifice (or several orifices) on the pads directly into the bearing clearance. As opposite to an active lubrication regime, in the hybrid regime the injection pressure is fixed to a constant value. By doing so, it is possible to modify the oil film pressure profile, entailing a modification of the dynamic properties of the TPJB [19–21]. Hence, it is reasonable to think that by using a proper configuration for the hybrid system it should be possible to extend the rotor stable operating range.

A number of configurations (defined by position of injection holes on the pads) were tested using the available model for the rotor-TPJBs system. From those preliminary iterations, two configurations were chosen and are presented here. They provide satisfactory results regarding to an increase of the rotor stability range. Both configurations set the position of the injection holes towards the leading edge of the bearing pads. A scheme for the disposition of the injection holes is provided in the figures. It is important to highlight that the distribution of the holes is not symmetrical with respect to the pivot line (no holes are positioned close to the trailing edge).

In Fig. 13, it can be seen that by injecting pressurized oil into the bearing clearance the equilibrium position of the rotor journal and the bearing pads is greatly influenced. By injecting oil near the leading edge of the pads, one increases the pressure field on that region. In order to achieve its static equilibrium, the pressure near the trailing edge must be incremented, hence a higher

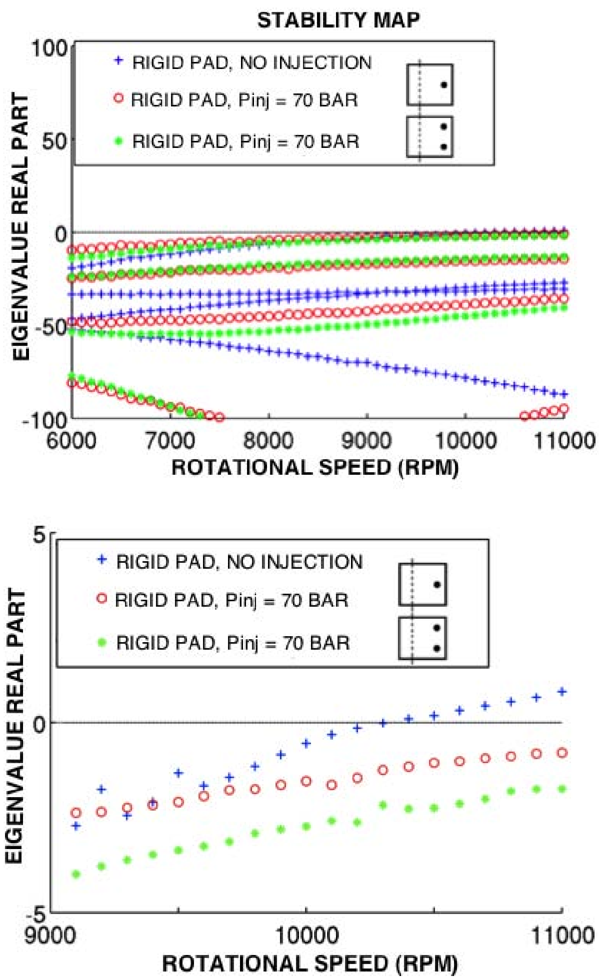

FIGURE 15. STABILITY MAP FOR THE COMPRESSOR; EFFECT OF HYBRID OIL INJECTION FOR TWO CONFIGURATIONS (LOWER FIGURE DETAILS THE INSTABILITY ONSET ZONE)

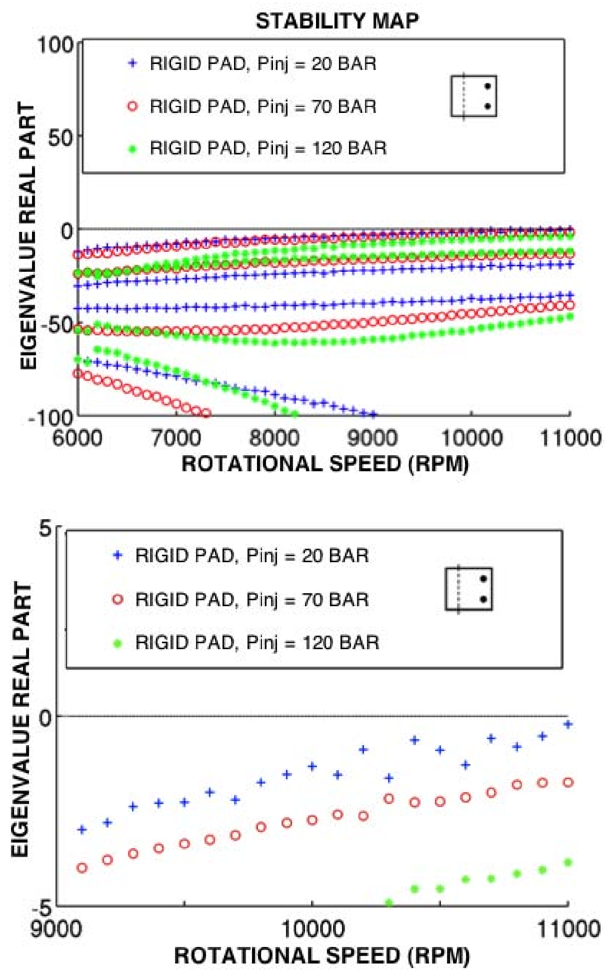

FIGURE 16. STABILITY MAP FOR THE COMPRESSOR; EFFECT OF INJECTION PRESSURE FOR HYBRID REGIME FOR “TWO HOLE“ CONFIGURATION (LOWER FIGURE DETAILS THE INSTABILITY ONSET ZONE)

tilt for the pads is observed. It can be seen that such effect is more pronounced forces for the “two injection holes“ configuration, which is consistent with the higher increase in the pressure field when compared to the ”one hole” configuration.

The corresponding change in the oil film thickness and pressure profile entails modification of the bearing dynamic coefficients, as can be seen in Fig. 14. It can be noted that the expected decrease in the damping for the TPJB when increasing the rotor rotational speed is actually diminished when using the hybrid lubrication regime. A reduction in damping is obtained for this regime when compared to the passive configuration (no injection), but the damping characteristics remain more or less constant through the analyzed rotational speed range.

When looking at the stability map depicted in Fig. 15, it can be seen that both configurations for the hybrid lubrication enable to extend the stable operational range of the rotor. Although it can be seen that the real part of the eigenvalues get closer to zero for the studied range when compared to the “no injection“ case, the instability onset speed is increased for the hybrid lubrication regime. As for the effect of the injection pressure, from Fig. 16, it can be seen that even for a relatively low injection pressure (20 bar), it is possible to increase the instability onset speed of the rotor, when compared to the passive lubrication regime. Hence, it has been demonstrated that the use of a hybrid lubrication regime, with the proper positioning of the injection holes on the pads, can present advantages over a passive regime (no injection) when considering the stability of the system. Another benefit from this regime is the cooling effect, reducing the overall temperature of the oil film [23, 24].

CONCLUSION

In this work, an industrial compressor mounted over TPJBs has been modeled and analyzed, in order to assess the effect of including different lubrication regimes in the dynamic behavior of the system. Results have been obtained in the form of equilibrium positions and dynamic coefficients for the TPJBs, and stability map for the compressor. According to the numerical results obtained, one can state the following conclusions:

1. The instability onsed speed of the rotor-TPJB system studied is: 10300 RPM for the passive bearing for isothermal model with no pad flexibility effects included; 9900 RPM for the THD lubrication regime; 10300 for the EHD lubrication regime; over 11000 RPM for the hybrid lubrication regime.
2. The results obtained for the stability map show that neglecting the temperature build up of the oil film due to viscous forces generated during the bearing operation would induce an overestimation of the instability onset speed for the rotor. Hence, according to these results, even for a rotor working with loading and speed conditions as the ones imposed on the model (which can be considered to be on the "low" range) it is relevant to include a THD modeling of the oil film behavior.
3. The inclusion of the pad flexibility effect into the modeling, using a pseudo modal reduction scheme, presented a negligible effect on the instability onset speed for the analyzed rotor, when compared to the results obtained when including the THD model. Again, such result must be analyzed taking into account the particular operational conditions of the analyzed rotor.
4. When analyzing the synchronously reduced dynamic coefficients for the TPJBs, it can be noted that the inclusion of the pad flexibility into the modeling induces an increase in the stiffness and a reduction on the damping of the bearing. Hence, a model for TPJB that neglects the pad flexibility will overestimate the damping of the bearing.
5. The results obtained for equilibrium positions and dynamic coefficients for the bearings and stability map for the rotor show that the effect of including higher modes into the pseudo modal reduction scheme is negligible when compared to just including the first bending mode for the pads. Convergence behavior is observed when including higher modes into the modeling. Hence, according to these results it is enough to include the first bending mode in order to model the effect of flexibility of the pads.
6. The results of the stability analysis of the rotor-TPJB system using the synchronously reduced dynamic coefficients showed an overestimation of the stable operating range of the rotor, when compared to the results obtained using the full set of dynamic coefficients.
7. The theoretical results obtained show that when imposing a hybrid lubrication regime for the bearings, using a constant oil injection pressure, it is possible to extend the stable operational range for the rotor. The results obtained are dependent on the configuration for the injection holes on the pad and the oil injection pressure. From the obtained results, it can be concluded that a proper configuration for increasing the instability onset speed of the rotor must place the injection holes towards the leading edge of the pads.

REFERENCES

[1] Glienicke, J., 1987. "Stabilitatsprobleme bei Lagerung schnellaufender Wellen - Berechnung, Konstruktion und Verhalten von Mehrflchen- und Kippsegmentlagern". *Technische Akademie Wuppertal, Germany*.

[2] Flack, R. D., and Zuck, C. J., 1988. "Experiments on the Stability of Two Flexible Rotor in Tilting Pad Journal Bearing". *Tribology Trans.,* ***31***(2), pp. 251–257.

[3] Lund, J., 1964. "Spring and Damping for the Tilting Pad Journal Bearings". *ASLE Trans.,* ***7***(4), pp. 342–352.

[4] Allaire, P., Parsell, J., and Barrett, L., 1981. "A Pad Perturbation Method for the Dynamic Coefficients of Tilting-Pad Journal Bearings". *Wear,* ***72***, pp. 29–44.

[5] Malcher, L., 1975. "Die Federungs- und Dampfungseigenschaften von Gleitlagern fur Turbomaschinen - Experimentelle Untersuchungen von MGF- und Kippsegmentlagern". PhD Thesis, Technical University of Karlsruhe.

[6] Klumpp, R., 1976. "Die Eigenschaften von Kippsegment-Radiallagern". *Konstruktion,* ***28***(8), pp. 320–324.

[7] Jones, G., and Martin, F., 1979. "Geometry Effects in Tilting Pad Journal Bearings". *ASLE Trans.,* ***22***(3), pp. 227–246.

[8] Springer, H., 1978. "Zur Berechnung Hydrodynamischer Lager mit Hilfe von Tschebyscheff-Polynomen". *Forsch. Ing.-Wes,* ***44***(4), pp. 126–134.

[9] Springer, H., 1979. "Nichtlineare Schwingungen schwerer Rotoren mit vertikaler Welle und Kippsegmentradiallagern". *Forsch. Ing.-Wes,* ***45***(4), pp. 119–132.

[10] Rouch, K., 1983. "Dynamic of Pivoted Pad Journal Bearings, including Pad Translation and Rotation Effects". *ASLE Trans.,* ***26***(1), pp. 102–109.

[11] Allaire, P., Parsell, J., and Barrett, L., 1983. "Frequency Effects in Tilting Pad Journal Bearing Dynamic Coefficients". *ASLE Trans.,* ***26***(2), pp. 222–227.

[12] Ettles, C., 1980. "The Analysis and Performance of Pivoted Pad Journal Bearings considering Thermal and Elastic Effects". *J. Lubr. Tech., ASME Trans.,* ***102***(2), pp. 182–194.

[13] Lund, J., 1987. "The Influence of Pad Flexibility on the Dynamic Coefficients of a Tilting Pad Journal Bearing". *ASME Journal of Tribology,* ***109***, pp. 65–70.

[14] Earles, L., Palazzolo, A., and Armentrout, R., 1990. "A Fi-

nite Element Approach to Pad Flexibility Effects in Tilting Pad Journal Bearings: Part I - Single Pad Analysis". *ASME Journal of Tribology,* ***112***, pp. 169–177.

[15] Earles, L., Palazzolo, A., and Armentrout, R., 1990. "A Finite Element Approach to Pad Flexibility Effects in Tilting Pad Journal Bearings: Part II - Assembled Bearing and System Analysis". *ASME Journal of Tribology,* ***112***, pp. 178–182.

[16] Dmochowski, W., 2007. "Dynamic Properties of Tilting-Pad Journal Bearings: Experimental and Theoretical Investigation of Frequency Effects due to Pivot Flexibility". *ASME Journal of Engineering for Gas Turbines and Power,* ***129***, July, pp. 865–869.

[17] Fillon, M., Bligoud, J. C., and Frêne, J., 1992. "Experimental Study of Tilting-Pad Journal Bearings – Comparison with Theoretical Thermoelastohydrodynamic Results". *ASME 1991 Modal Analysis, Modeling, Diagnostics and Control – Analytical and Experimental,* ***114***, pp. 579–588.

[18] Santos, I., 1994. "Design and Evaluation of Two Types of Active Tilting Pad Journal Bearings". In *The Active Control of Vibration*, C.R.Burrows and P.S.Keogh, eds. Mechanical Engineering Publications Limited, London, England, pp. 79–87.

[19] Santos, I., 1995. "Strategien fur die Erhohung der Dampfungsreserve von kippsegmentgelagerten Rotorsystemen". In *Schwingungen in rotierenden Maschinen*, H. S. H. Irretier, R.Nordmann, ed., Vol. 3. Vieweg Verlag, Braunschweig, Germany, pp. 3–12.

[20] Santos, I., 1997. "Aktive Schmierung zur Regelung von Rotorsystemen". In *Schwingungen in rotierenden Maschinen*, H. S. H. Irretier, R.Nordmann, ed., Vol. 4. Vieweg Verlag, Braunschweig, Germany, pp. 37–47.

[21] Santos, I., and Russo, F., 1998. "Tilting-Pad Journal Bearings with Electronic Radial Oil Injection". *Journal of Tribology, ASME Trans.,* ***120***(3), pp. 583–594.

[22] Lund, J., 1974. "Stability and Damped Critical Speeds of a Flexible Rotor in Fluid-Film Bearings". *ASME Trans.,* ***73***, pp. 509–517.

[23] Santos, I., and Nicoletti, R., 1999. "THD Analysis in Tilting-Pad Journal Bearings using Multiple Orifice Hybrid Lubrication". *Journal of Tribology, ASME Trans.,* ***121***, pp. 892–900.

[24] Santos, I., and Nicoletti, R., 2001. "Influence of Orifice Distribution on the Thermal and Static Properties of Hybridly Lubricated Bearings". *International Journal of Solids and Structures,* ***38***, pp. 2069–2081.

[25] Kim, J., Palazzolo, A., and Gadangi, R., 1995. "Dynamics Characteristics of TEHD Tilt Pad Journal Bearing Simulation including Multiple Mode Pad Flexibility". *ASME Journal of Vibration and Acoustics,* ***117***(1), January, pp. 123–135.

[26] Haugaard, A., and Santos, I., 2010. "Multi-orifice Active Tilting-Pad Journal Bearings-Harnessing of Synergetic Coupling Effects". *Tribology International,* ***43***(8), pp. 1374–1391.

[27] Haugaard, A., and Santos, I., 2010. "Stability of Multi Orifice Active Tilting-Pad Journal Bearings". *Tribology International,* ***43***(9), pp. 1742–1750.

[28] Nelson, H., and McVaugh, J., 1976. "The Dynamics of Rotor-Bearing Systems Using Finite Element". *J. Eng. Ind.,* ***98***, pp. 593–600.